REACTIONS IN SOLID PHASE—I

KARTAR SINGH

Defence Science Laboratory, Delhi

(*Received* 23 *February*, 1966)

The chemical reactivity in solids results from imperfections in electronic distribution in bands and point or line imperfections in atomic arrangement. The ease with which these imperfections are formed and move within the crystal influences the speed of the reactions. The properties of these imperfections are derived from the study of electronic and ionic conductivity, spectroscopy, X-ray diffraction and luminescence. With precise information about the nature of defects it is possible to control the reactivity of solids. The importance of these studies in extending the knowledge of solid state and in improving industrial applications has been highlighted.

The study of chemical reactions in solid phase is proving very rewarding. It is extending our knowledge of behaviour of imperfections in solids. It is valuable in the development of new materials, electronic devices and integrated circuits. It is proving useful in modification of the properties of primary explosives. Out of the vast field, it is proposed to cover only those aspects which are of importance in theory and practice. The topics covered include

(*i*) Application of activated complex theory to the decomposition in solid phase

(*ii*) Band theory and imperfections in solids

(*iii*) Photographic sensitivity and radiolysis

(*iv*) Chemical reactivity in solids

and (*v*) Catalyst

Oxidation of metals is discussed in Part II. An attempt has been made to present a coherent account of these topics rather than detailed survey.

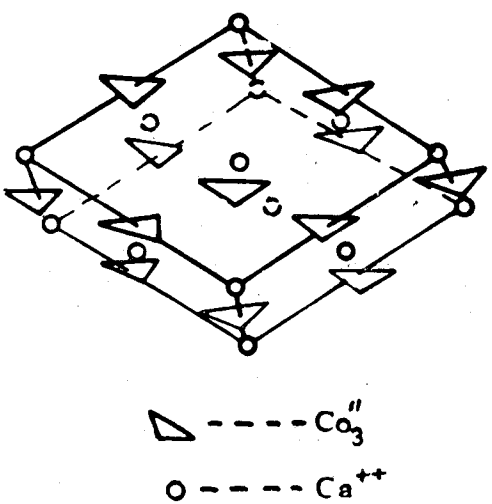

FIG. 1—Structure of calcite

APPLICATIONS OF ACTIVATED COMPLEX THEORY TO THE REACTIONS IN SOLID PHASE

For the application of the theory of rate processes to solid phase reactions it is necessary to have a model of the activated complex involved in the reaction. Reliable data exist in the case of decomposition of calcite in vacuum which proceeds at the interface between the crystal and the gaseous product. Calcite possesses a rhombohedral structure as shown in Fig. 1. Each planar CO_3^{--} group possesses six nearest neighbours of Ca^{2+} ions.

The transition complex may be assumed to have the structure $Ca—O—CO_2$ as shown in Fig. 2. The equation of absolute rate theory is

$$K_r = \frac{kT}{h} \cdot \frac{F^*}{F} \cdot \exp\left(\frac{-E}{kT}\right) \quad (1)$$

where K_r is first order rate constant, F and F^* are complete partition functions for the reactant and activated complex respectively, k is Boltzmann's constant, T is temperature in degrees absolute, h is Planck's constant and E is activation energy for the process. In calculating F's it may be assumed that at the temperature of decomposition, CO_3 group undergoes complete rotation. The lattice vibrations in solids are analogues of translational degrees of freedom in gaseous state. Accoustic modes which involve movement of unit cells against each other may not be effective in chemical reaction. The internal vibrations of atoms within the group, rotations of CO_3 group about two fold axes and optically active lattice modes contribute towards partition function which is given by the expression

$$F = f^3{}_L \cdot f^3{}_{(\text{rot})} \cdot f^6{}_{(\text{vib})} \quad (2)$$

where $f^3{}_L$ is partition function for three optically active lattice modes of vibration $\nu_1{}^L = 367\ \text{cm}^{-1}$, $\nu_2{}^L = 330\ \text{cm}^{-1}$ and $\nu_3{}^L = 106\ \text{cm}^{-1}$; $f^3{}_{(\text{rot})}$ is partition function for three rotations of CO_3 group and $f^6{}_{(\text{vib})}$ is partition function for six internal vibrations

$$\nu_1{}^i = \nu^i{}_2 = 712\ \text{cm}^{-1},\ \nu_3{}^i = \nu_4{}^i = 1461\ \text{cm}^{-1}$$
$$\nu_5{}^i = 881\ \text{cm}^{-1} \text{ and } \nu_6{}^i = 1070\ \text{cm}^{-1}$$

For calculation of the partition function of the activated complex, the following properties may be assigned to the complex (*i*) CaO is a part of the crystal lattice (*ii*) CO_2 group is attached to CaO and is rotating in xy plane, (*iii*) CO_2 group oscillates in direction perpendicular to xy plane, (*iv*) the order of bond in $(Ca\ O)—(CO_2)$ system is 1/2. On the basis of these assumptions partition function for the activated complex is given by the expression

$$F^x = f^3{}_L\ f^2{}_{L'}\ f^1{}_{(\text{rot})}\ f^4{}_{(\text{vib})} \quad (3)$$

here $f^3{}_L$ is partition function for three lattice vibrations of CaO group ${}^x\nu_L = 690\ \text{cm}^{-1}$, ${}^x\nu_L = {}^y\nu_L = 364\ \text{cm}^{-1}$, $f^2{}_{L'}$ is partition function for two lattice vibrations of $(CaO)—(CO_2)$ system, ${}^x\nu_{L'} = {}^y\nu_{L'}$, $= 350\ \text{cm}^{-1}$, $f^1{}_{rot}$ is partition function for rotation of CO_2 group and $f^4{}_{vib}$ is partition function for four vibrations of CO_2 group ${}^1\nu_{vib} = 1345\ \text{cm}^{-1}$, ${}^2\nu_{vib} = {}^3\nu_{vib} = 667\text{cm}^{-1}$ and ${}^4\nu_{vib} = 2349\ \text{cm}^{-1}$. From the infra-red and Raman data on $CaCO_3$, $Mg\ O$, CO_2 deposited on $AgCl$ plate, solid CO_2 and assumed bond order of $(CaO)—(CO_2)$ system, suitable values may be assigned to various vibrations. On these assumptions, partition functions may be calculated. Shannon[1] has estimated the value of $\frac{F^*}{F} = a = 0{\cdot}4 \times 10^{-2}$ which compares favourably with experimental value of $0{\cdot}6 \times 10^{-2}$.

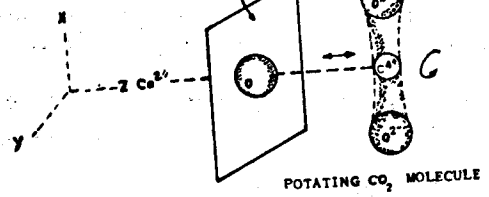

FIG. 2—Structure of activated complex

Point imperfections play a dominant role in solid phase reactions. The theory of rate processes ignores their existence. It has to be suitably modified to take account of their presence.

BAND THEORY AND IMPERFECTIONS IN SOLIDS

Electronic processes in solids are greatly influenced by electron distribution in the periodic field within solids. The band structure is a direct consequence of the close proximity of atoms in the lattice. If there are N atoms in the lattice, each level in the isolated atom is split into N sublevels which constitute a band. The energy levels of these sublevels can be deduced by making use of the Bloch function

$$\psi_{k_\omega} = u_{k_\omega} \cdot e^{ik_\omega \cdot r} \tag{4}$$

where k_ω is a wave vector, u_{k_ω} is a periodic function and r is distance from the origin. It may be assumed that if $k_\omega = 0$, $\psi = u_\circ$. As an approximation, the Bloch function may be assumed to have the form

$$\psi = u_\circ \cdot e^{ik_\omega \cdot r} \tag{5}$$

This function gives the following expression for the Eigen-values of the sublevels

$$E = \frac{\hbar^2}{2m} \cdot k^2_\omega + E_\circ \quad \ldots\ldots \tag{6}$$

where $\hbar$ is equal to $\frac{h}{2\pi}$, and m is mass of the electron. This expression gives approximate shape of the curve representing energy versus wave vector k_ω.

It is interesting to establish the band structure for a typical crystal lattice say silver chloride. Photo emission[2] gives value of work function φ_ω which is the energy required to excite an electron from the top of the full band to infinity. Optical and photo[3] conductivity data give width of forbidden band E_g. The energy required to remove an electron from valence band to silver nuclei or threshold of Hershel[4] effect is found to be $h\nu = \phi_\omega - \chi$ where ϕ_ω is work function of silver 4·7 ev, and χ is electron affinity of the crystal. Gilleo has given[5] a value of 1·1 ev for photo emission from silver into large single crystal of silver chloride at 80° K.

The width of the chloride band may be calculated by making use of linear combinations of Bloch sums built up from 3 p orbitals on chloride ions within unit cell. The effect of metal ions may be neglected. Howland[6] has shown that chloride band may have a width of about 1 ev. He has suggested that a branch of the valence band bends upwards towards a maximum which may not be at $k_\omega = 0$ at least along one crystallographic axis. This effect may be more pronounced in silver chloride.

The study of magneto-conductivity[7] gives information about symmetry elements in band structure. In case of crystals of cubic symmetry having standard band shape, the fractional change in conductivity $\frac{\triangle(\sigma)}{\sigma(o)}$ in presence of magnetic field H is given by the expression

$$\frac{\triangle\sigma}{\sigma(o)} = -\frac{\gamma H^2 \cos^2\theta}{\sigma(o)} \qquad (7)$$

where θ is the angle which magnetic field H makes with the direction transverse to the direction of electric field and γ is coefficient giving effect of magnetic field on current. An agreement of the experimental results with those calculated from expression (7) suggests that conduction band in silver chloride is of standard form with minimum centred at $k_\omega=0$.

The optical absorption[8] provides information regarding the band structure. The first absorption peak at 250 mμ in silver chloride corresponds to excitation of an electron on chloride ion. The excitation peak is a usual doublet. The absorption in the tail of the absorption peak produces photo-conductivity. Indirect transition assisted by phonons which help in conservation of wave vector may be responsible for this absorption. It is for this reason that threshold of absorption shifts to higher energies as the temperature is lowered. These results indicate that vertical transition near $k_\omega=0$ occurs at about 5·1 ev.

Based upon these observations a hypothetical[9] band structure shown in Fig. 3 may be assigned to silver chloride. Here energy is shown as a function of wave vector $k_\omega=2\pi/\lambda$.

The conduction band Γ_1 has the standard form $E = \frac{\hbar}{2m} k^2_\omega$ near $k_\omega = 0$. Valence band Γ_{15} is composed of 3 p states of chloride ions. Bands Γ_{12} and Γ_{25} may be due to 4 d states of silver ions.

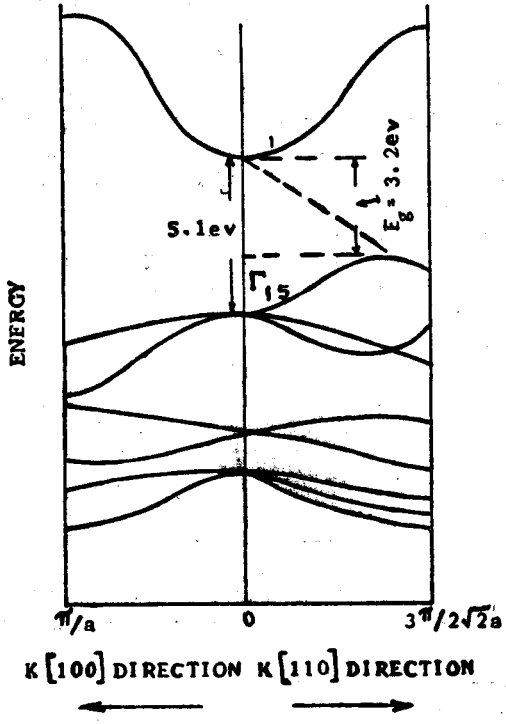

FIG. 3—Hypothetical band structure of AgCl

Perfect band structure may be disturbed by excitation of an electron ($\bar{e}$) from the valence band to the bottom of the conduction band. As a result of this a hole h^+ may be left behind. Dissociation of electron and hole may not be complete. A pair of electron and hole bound together by Coulomb forces constitutes a Mott excitaton. Frenkel exciton may be identified as an excited atom or ion in the lattice. The excitons may be transmitted to neighbouring atoms or ions of the same kind. They dissociate into free valencies on collision with phonons.

Imperfections which influence the reactivity of solids include vacancies, interstitials, impurity atoms and dislocations. A short review on the formation of these imperfections is given by Dekeyser[10]. In the present discussion symbols Ai and $\square_B$ denote atom A at interstitial position and a vacancy at site B respectively. A cross, dash or dot

on symbol for imperfection indicates neutral, negative or positive charge. The impurity atoms may act as acceptors or donors. As for example interstitial copper ions in lead sulphide act as donors but copper ions at lattice sites in lead sulphide serve as acceptors. Dislocation play an important role in the formation or annihilation of interstitials and vacancies.

Various types of colour centres may play an important part in reactions in solid phase. Models of various centres are shown in Fig. 4. F centre comprises an anion vacancy and a trapped electron. R_1 and R_2 centres consist of two negative vacancies with respectively one or two trapped electrons. M centre is made up of a F centre and a pair of vacancies of opposite sign. Z centre is an divalent ion with trapped electron. V centres play a dominant role in solid phase reactions and are discussed below.

Christy and Phelps[11] have investigated the structure of V centres in potassium chloride. According to them H centre is associated with molecular ion Cl_2'. It is oriented in [110] direction and it is located at a vacant anion site. In the presence of divalent impurity, this centre assumes a different character, Cl_2' ion in the new centre tends to lie in [100] instead of [110] direction. On association of another anion vacancy with H centre, molecular bond in Cl_2' ion is stabilized and the H centre transforms into V_k centre. H centre by trapping another hole becomes V_1 centre. This centre may be associated with Cl_2 molecule which may be located at the site of an anion vacancy. The centre is non-magnetic in nature. A hole may be trapped on three chlorine ions in presence of two cation vacancies and one anion vacancy. The centre formed in this way is called V_4 centre. It is associated with the $(Cl_3)^{-2}$ ion. The details of this centre have been studied by Cohen, Kanzig & Woodruff[12].

V_3 centre consists of two holes shared by three chlorine ions $(Cl_3)'$ The complex-ion is oriented in [100] direction. It is stabilized by the presence of the cation vacancies and one anion vacancy. It is non-magnetic in nature and is stable at room temperature. V_2 centre has some relationship with V_3 centre. It is transformed into the latter on

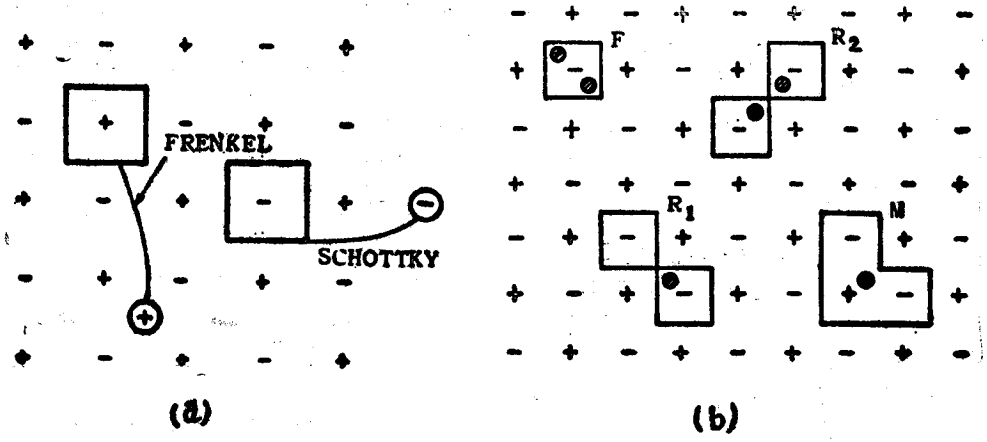

FIG. 4 (*a*)—Schottky and Frenkel defects in an ionic crystal. The arrows indicate the direction of displacement of ion and (*b*) The F' centre is obtained on adding a second electron to an F centre. The R_1 centre has one electron associated with the anion vacancies and the R_2 centre is obtained on adding a second electron to R_1 centre. M centre has one electron bound to two anion vacancies and one cation vacancy.

warming from low temperature. The absorption peaks observed at 215, 230, 255, 345, 355 and 365 mμ in potassium chloride have been assigned to V_3, V_2, H, V_1 and V_k centres respectively.

The presence of these centres, and dislocations which are line imperfections add to the reactivity of solids. A typical case of silver bromide is discussed below.

Recent investigations show that silver bromide possesses predominantly Frenkel disorder[13,14] which consists of cation vacancies and interstitial silver ions. Calculations by Kroger[15] show that Schottky disorder does not become dominant in silver bromide. Self-diffusion of bromine has to be explained by assuming diffusion via silver ion vacancies. A hole trapped by silver ion vacancy in silver bromide under a pressure of bromine gives rise to defect centre $\square^{+}_{Ag}$. It is estimated that concentration of these centres in silver bromide reach a value of 10^{-4} atomic fraction at temperatures above 300°C.

The concentration of electrons and holes in silver bromide can be represented by means of the expression

$$\left[h^{+}\right]\left[\bar{e}\right] = C_i \exp\left(\frac{-E_i}{kT}\right)\left(\text{mole } fr\right)^2 \qquad (8)$$

where C_i is a constant. Expression (8) can be derived from consideration of the equilibria

$$\tfrac{1}{2}Br_2 \rightleftharpoons Br'_{Br} + \square_{Ag} + h^{+} \qquad (9)$$

$$Ag(s) + V_i \rightleftharpoons Ag_i^{+} + \bar{e} \qquad (10)$$

where V_i is a vacant interstitial site and (s) implies solid state. The concentration of holes h^{+} can be determined by study of conductivity of the hole rich sample which is obtained by subjecting silver bromide to a vapour of bromine[16]. The electron concentration is determined by investigating the electronic conductivity of silver bromide in equilibrium with silver. For this purpose polarization[17] studies on the cell $Ag/Ag\,Br/Pt$ are carried out. Kroger's estimate gives $C_i = 3\times10^5$, and $E_i{}^0 = 3{\cdot}38$ ev. These results compare favourably with the deductions of band theory which gives the relationship[18]

$$\left[e\right]\left[h^{+}\right] = k_e = g_c\ g_v\ A_e\ A_h \exp\frac{-(E_i{}^\circ - \beta T)}{kT} \qquad (11)$$

where g_c any g_v are the number of valleys in the conduction and valence bands respectively

$$A = \left(\frac{2\pi\ m^*\ kT}{h^2}\right)^{3/2}$$

Here m^* is effective mass of electron or hole.

$$g_e = 1,\ g_v = 12,\ m_e = 0{\cdot}27,\ m_h = 1,$$
$$E_1{}^\circ = 3{\cdot}38\ ev \text{ and } \beta = 1{\cdot}9 \times 10^{-3}\ ev/T \text{ for silver bromide.}$$

Layer & Slifken[19] have studied the existence of excess point defects in samples of silver chloride subjected to pulsed plastic extension and thermal treatment involving heating to high temperature followed by cooling. They have found that interstitial silver ions produced above the equilibrium concentration have a life of 10^8 jumps. They have also estimated that rapid cooling of silver chloride quenches in approximately 0·1% Schottky defects. The positive and negative vacancies exist in pairs. The divacancies have activation energy of 23·00 k calories for migration and of 9·8 k. calories for dissociation.

Lattice vibrations increase entropy of solid which results in the formation of point defects. The mechanism of formation of Frenkel defects in silver bromide is discussed below. Similar remarks apply to the formation of Schottky, defects. In a crystal containing N lattice sites and N' interstitial positions, the number of Frenkel defects (n_F) is given by the expression

$$n_F = \sqrt{N_l\, N'} \exp\left(\frac{-g_F}{2kT}\right) = \frac{1}{k_i} \tag{12}$$

where $g_F = u_F - Ts_F$ is free energy of formation of Frenkel defect, u_F is enthalpy and s_F is entropy of the formation of the defect. With the help of the relationship (12), it is possible to derive the expression.

$$u_F = \frac{\partial \log k_i}{\left[\partial\left(\frac{1}{kT}\right)\right]_P} \tag{13}$$

Various parameters in equation (12) can be determined by study of anomalous expansion $\triangle V$ and anomalous specific heat $\triangle C_P$. These two properties are associated with increase in number of defects with rise in temperature as shown below:

$$\triangle V = n_f \,.\, v_f \tag{14}$$

$$\left(\frac{\partial \triangle V}{\partial T}\right)_P = v_f\, u_f \frac{\sqrt{N_l \,.\, N'}}{2kT^2}\, e^{\frac{-g_F}{2kT}} \tag{15}$$

$$\triangle C_P = \frac{u^2_F}{2kT^2} \sqrt{N_l\, N'}\, e^{\frac{-g_F}{2kT}} \tag{16}$$

where v_f is free volume of formation of the defect. By making use of expressions (15) and (16) and measured[20, 21] values of $\triangle V$, $\left(\frac{\partial \triangle V}{T}\right)_P$ and $\triangle C_P$ it is possible to derive concentration $\frac{n_f}{N_l}$ of defects which may be represented by the expression[22]

$$\frac{n_f}{N_l} = 1600 \exp \frac{-14{,}700}{RT} \tag{17}$$

where R is a gas constant in calories/degree. The heats of formation u_F and migration u_m of defects can be derived from conductivity σ data which may be represented in the form

$$\sigma = \frac{a^2 e^2}{kT} \sqrt{N_l N'} \exp \frac{-(g_m + g_F)}{2kT} \tag{18}$$

$$u_m + \tfrac{1}{2} g_F = - \frac{\partial (\log \sigma T)}{\left[\partial \left(\frac{1}{kT}\right)\right]_P} \tag{19}$$

where a is the distance between nearest similar atoms and g_m is free energy of migration of defects and e is electronic charge, and σ is specific conductivity. Shapiro & Kolthoff's[23] data on intrinsic conductivity of silver bromide can be represented in the form

$$\sigma = 3 \times 10^5 \exp \frac{-18{,}000}{RT} \tag{20}$$

TABLE 1

DEFECT CONCENTRATION AT VARIOUS TEMPERATURES

Temp. °C	χ_m	Mole % x_o	v_f cm³ Frenkel defect
175	7	0·004	16·00
350	2	0·400	

and the low temperature data by the expression

$$\sigma = A_1 \exp \frac{-8{,}300}{RT} \tag{21}$$

The structure sensitive parameter A_1 varies from 0·20—25 depending upon the method of preparation of the sample. Further information may be derived from the study of doped samples.

From the plots of conductivity σ versus concentration c of dopant $Cd\ Br_2$ it is possible to derive mobility of interstitial ions. Study of variation of concentration of interstitials with pressure p makes it possible to derive the free volume v_f of defect. For determination of v_f, use is made of the relationship

$$\left(\frac{\sigma}{\sigma_o}\right)_{min} = \frac{2\sqrt{\chi_m}}{(1+\chi_m)} \tag{22}$$

$$\left(\frac{\sigma}{\sigma_o}\right) = \left[\left(\frac{c}{2x_o}\right)^2 + 1\right]^{1/2} - \frac{c}{2x_o} \cdot \frac{\chi_m - 1}{\chi_m + 1} \tag{23}$$

$$\frac{\partial \log x_o}{\partial P} = -\frac{1}{2kT} \cdot \frac{\partial g_F}{\partial P} = -\frac{v_f}{2kT} \tag{24}$$

where χ_m is ratio of interstitial mobility to vacancy mobility, $x_o = n_f / N$ is concentration of defects in pure silver bromide, $(\sigma/\sigma_o)_{min}$ is minimum value of ratio of conductivity of the sample to the conductivity of pure silver bromide. The molar volume of silver bromide is 29 cm.³ Typical values of various parameters are given below[24,25].

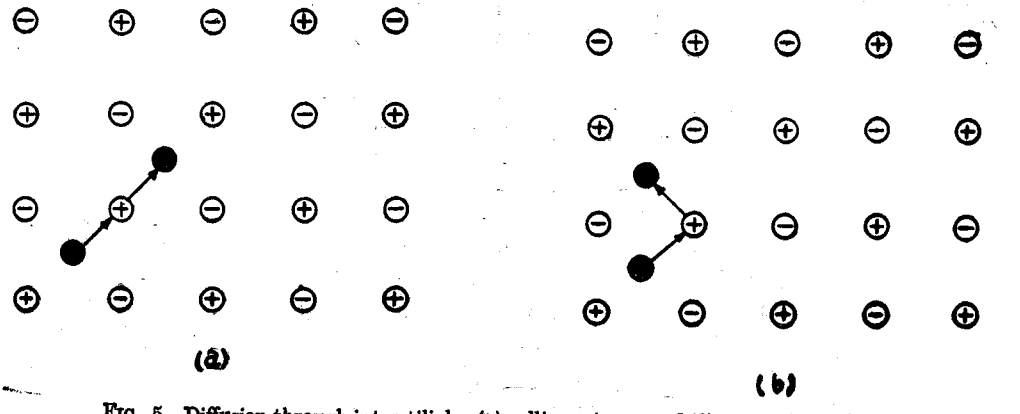

FIG. 5—Diffusion through interstitialcy (a) collinear jump and (b) non-collinear jump.

The chemical reactions in solids depend upon mass transport through lattice. The diffusion occurs as a result of migration of vacancies, divacancies and interstitials under gradient of concentration and field effect. The Frenkel defects may also migrate through interstitialcy mechanism. In a typical case of diffusion involving interstitial ions, the diffusion coefficient is given by the expression

$$D = \wedge \lambda^2 n_i \nu e^{-E_m/kT} \tag{25}$$

where $\wedge$ is a factor giving probability that a point defect is in a position to diffuse, λ is a distance between jump sites, ν is atomic vibration frequency, n is fractional concentration of defects and E is activation energy for diffusion. In interstitialcy mechanism an interstitial ion knocks out an ion from the lattice site and occupies the site so vacated. The jump may be collinear or non-collinear as shown in Fig. 5. The nature of jumps can be decided by studying the relationship between coefficient of diffusion D and conductivity σ

$$\sigma/D = BN_i e^2/kT \tag{26}$$

where N_i is concentration of atoms of one kind, B is correlation coefficient, e is electronic charge, B is equal to 1·273 and 1·38 in case of vacancy diffusion, collinear and non-collinear interstitialcy mechanisms respectively. Direct jumps of interstitial ions to vacant interstitial sites involves no correlation effect. The values of B has been derived by McCombie & Lidiard[26].

Recent investigations by Friauf[27] indicate that diffusion in silver bromide involves both collinear and non-collinear interstitialcy jumps. The large mass transfer is made possible by high mobility of interstitial silver ions and low activation energy required for collinear interstitialcy mechanism.

For diffusion in diamond type structure the choice is between vacancy or interstitial mechanism. Interstitialcy mechanism is ruled out as it involves very high activation energy. In diamond structure the bonds are directed towards the corners of a tetrahedron and there are open spaces in between. The geometry of diffusion of an interstitial atom is shown in Fig. 6. In order to get from one interstitial site to the next, the impurity atom must pass through a pickered hexagon with host atoms at the corners. Since extension of bonds of the hexagon involved is limited the activation energy is small. The mechanism of the diffusion of vacancy in diamond type of structure is shown in Fig. 7. As the shaded atom in Fig. 7 moves from one position to the next, the bonds joining it to the neighbours are bent and stretched. At transition state the bonds are stretched by 54·5% and are bent through 27·8°. The activation energy depends upon the energy required for distortion minus the energy involved in relaxation. A comparison of the magnitudes of activation energies shows that mechanism involving migration of interstitial[28] atoms is favoured in diamond type structures.

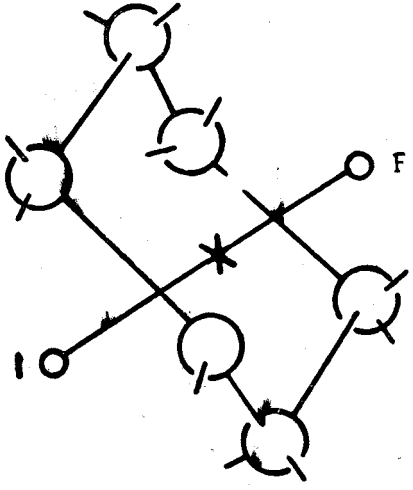

FIG. 6—Puckered hexagon barrier to interstitial migration in the diamond structure

Diffusion controlled reaction between particles of MgO and SiO_2 has recently been studied by Brindley & Hayami[29]

$$2\ MgO + SiO_2 \longrightarrow Mg_2\ SiO_4 \qquad (27)$$

The progress of reaction has been followed by X-ray diffraction, cathode luminescence and X-ray emission. The intensity of lines from fosterite $Mg_2\ SiO_4$ increases with time. In cathode luminescent image MgO appears bright blue, fosterite as brick red, enstatite $MgSiO_3$ as brilliant violet and silica as black. Electron probe technique gives intensity of $K\alpha$ lines from Mg and Si. Fosterite appears bright under crossed Nicols. These studies give the phase sequence

$$SiO_2 \mid MgO \quad SiO_2 \mid 2\,MgO \quad SiO_2 \mid MgO$$

in reaction layer.

In a spherical particle with radius R, the fraction α of reacted material may be written as

$$\left(1 - \frac{2}{3}\,\alpha\right) - (1-\alpha)^{2/3} = \frac{k_f \cdot t}{R^2} \qquad (28)$$

The variation of k_f with temperature gives activation energy of 78 k calories per mole. The rate controlling step is diffusion of Mg^{2+} through enstatite layer. Highly charged ions Si^{4+} are less free to migrate than divalent Mg^{2+} ions. Structure of SiO_2 is open whereas in MgO anions are closely packed. The evidence from theory and experiments is in favour of migration of Mg^{2+} ions into SiO_2. Experimental[30] data on reactions between Al_2O_3 and MgO are found to fit into equation for diffusion

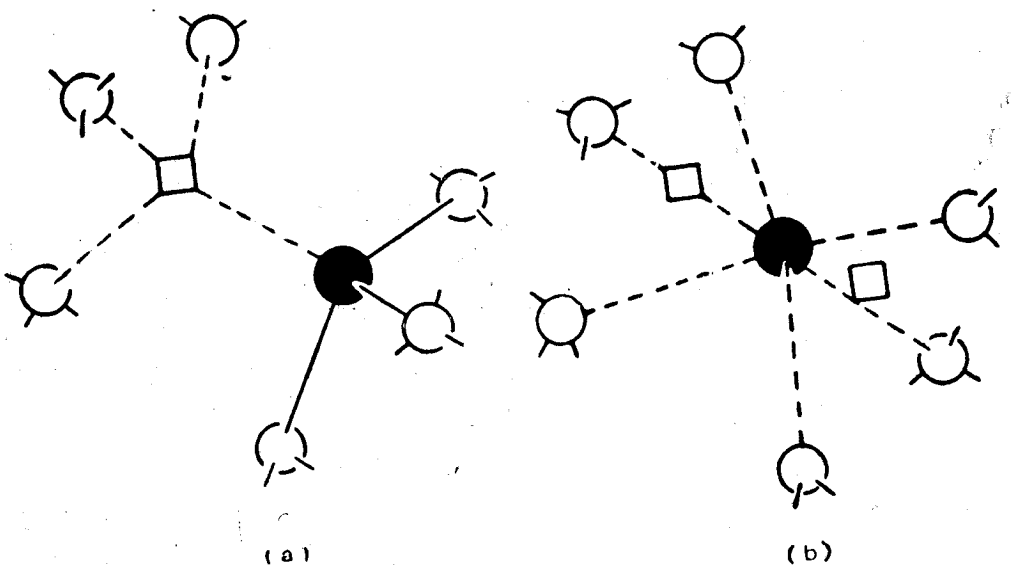

FIG. 7—Diffusion through vacancy in diamond structure (*a*) initial position [● — the moving atom □ —vacancy] (*b*) actuated position [●—The moving atom ; □—vacancy]

$$(1-\alpha) = \frac{6}{\pi^2} \sum_n \frac{1}{n^2} \exp(-n^2 k t) \qquad (29)$$

where k_f is reaction rate constant.

Photographic sensitivity and radiolysis

Recent investigations on photographic sensitivity have thrown ample light on mechanism of decomposition of silver bromide under the influence of light. The primary step is the excitation of an electron across the energy gap giving rise to free electron and hole in the lattice. In an ideal pure crystal electrons and holes recombine and there is the restoration of the order without any decomposition. Sensitization of the crystal can be achieved by immersion in a solution of sodium thiosulphate followed by washing. By this treatment Ag_2S is incorporated in the surface of the crystal in the form of monomolecular layer. Sensitization can also be achieved by plastic deformation[31] when large number of dislocations are generated along certain planes. Separation of silver nuclei and halogen in a sensitized crystal on illumination can be described in terms of Mitchell[32] or Gurney-Mott mechanism[33].

In chemically sensitized crystal electron trap X may be assumed to be silver ion near the sensitivity speck which is a portion of the absorbed monolayer of Ag_2S molecules. The hole may be trapped at another portion Y of the layer. According to Mitchell theory a hole is trapped by Ag_2S. The capture results in the formation of a diatomic AgS molecule and an adjoining cation vacancy.

$$Ag_2S + \text{hole} \longrightarrow Ag\,S + Ag^+ + \square_{Ag} \qquad (30)$$

Mechanism of decomposition may be visualized as follows:

$$\left.\begin{array}{l} O \longrightarrow \overset{+}{h} + e \xrightarrow{Y} \overset{+}{h} + (\overset{'}{\square}_{Ag} Y) \\ \overset{+}{Ag}_{Ag} \longrightarrow \overset{+}{Ag}_i + \overset{'}{\square}_{Ag} \xrightarrow{X} \overset{-}{e} + (\overset{+}{Ag}_i\ X) \end{array}\right\} \rightarrow \begin{array}{l} \overset{'}{\square}_{Ag}.\ \overset{+}{Y} \xrightarrow{\bar{B}_r} B_r \\ \overset{+}{Ag}_i . \overset{-}{X}) \longrightarrow \text{Silver speck} \end{array} \qquad (31)$$

The silver ion near the sensitivity speck $\overset{+}{Ag}_i X$ captures an electron and forms a free atom. The capture of another hole by Ag_2S is followed by capture of an electron by another silver ion near the sensitivity speck. The two atoms of silver set free form into a pair. In the similar manner a third atom may appear at this site. The three atoms may form into a triangle. An aggregate of more than three atoms forms a latent image which is fairly stable. This statement is supported by the observation that a sensitive grain of emulsion is made developable by absorption of four quanta of light.

In the Gurney-Mott mechanism an electron is trapped by sensitivity speck. The negative charge is neutralized by capture of an interstitial silver ion. A repetition of this process occurs three or four times when a stable latent image is formed. This mechanism may be represented by the equation.

$$\begin{array}{l} O \longrightarrow \overset{+}{h} + \overset{-}{e} \xrightarrow{X} \overset{+}{Ag}_i + \bar{X} \longrightarrow (\overset{+}{Ag}_i\ \bar{X}) \longrightarrow \text{Silver speck} \\ \overset{+}{Ag}_{Ag} \longrightarrow \overset{+}{Ag} + \overset{'}{\square}_{Ag} \xrightarrow{Y} Y + \overset{'}{\square}_{Ag} \longrightarrow (\overset{'}{\square}_{Ag} \overset{+}{Y}) \xrightarrow{\bar{B}_r} Br \end{array} \qquad (32)$$

In a sample which has undergone plastic deformation an electron may be trapped by silver ion which is present at the jog site along edge component of the dislocations. The hole may be captured by bromide ion on the surface or on internal sites at dislocation. As a result the halogen atom may be liberated which may combine with another halide ion. A new Br_2^- centre is formed. A second hole may be trapped at this centre. Br_2 molecule may subsequently escape from the surface. The jog sites, by successive trapping of electrons and silver ions, may lead to the formation of silver speck. Mechanism of radiolysis of salts containing polyatomic molecules is more complex.

Cunningham[34] has recently studied the radiolysis of alkali nitrates. He has determined G values which are slopes of lines representing formation of nitrate ions with dose of radiation. He has found ratio of G values for $K_{N^{14}O_3^{18}} / K_{N^{14}O_3^{16}}$ equal to 1·03 and 1·12 at —110°C and 25°C respectively. G may be assumed to be proportional to the probability of diffusion of oxygen fragments from excited NO_3^- through the cage of surrounding ions after it has been excited by radiation into repulsive state having maximum amplitude. The relationship may be put in the form

$$G \simeq D = \tfrac{1}{2}\, m\, \bar{\nu}\, (\triangle x)^2\, exp\, \left(\frac{-V_1}{k\,T}\right) \qquad (33)$$

where m is number of independent paths, $\bar{\nu}$ is weighted mean frequency of the lattice vibrations, V_1 is energy required to hold the neighbours from path of diffusion, $\triangle x$ is the distance of jump. In the frozen state at —110°C the exponential factor in expression (33) becomes unity. In the case of an excited and rotating ion, $\triangle x$ may occur in any direction within spherical volume around the nitrate ion. In view of this, the probability that an outgoing oxygen species may acquire amplitude $\triangle x$ for separation is dependent on available free space. G may for this reason be proportional to (free space)$^{\frac{3}{2}}$. This is consistent with experimental results.

The plot of *log G versus* $1/T$ above the temperature at which rapid enhancement of diffusion occurs provide estimate of V_1. The enhanced diffusion of oxygen fragment occurs as a result of favourable configurations of the cage for its outward motion. Increased vibrational amplitudes of units of the cage help in attaining the favourable configuration. This assumption is reasonable as a tightly bound lattice gives high value of V_1. Again relative rates k_r of reaction in NO_3^{18} and NO_3^{16} are given by the expression

$$\frac{k_r\ (16)}{k_r\ (18)} = \frac{f_{16} \cdot f^*_{18}}{f^*_{16} f_{18}} \left(\frac{E - \epsilon_{16}}{E - \epsilon_{18}}\right)^{n_v} \qquad (34)$$

where f and f^* are partition functions of the ground and excited states respectively, n_v is number of modes of vibartion of the ion, E is the energy given to the ion and ϵ_i is activation energy. Expression (34) gives isotopic effect of about 4%. The experimental value for the ratio k_r (16)/k_r (18) is 1·03 at —110°C which agrees with the above estimate.

Rise in temperature increases $\triangle x$ and provides additional paths. Both these factors increase G. Deactivation of excited species by collison with lattice atoms tends to reduce G. The jump rate across the same energy barrier favours the light isotope. The ratio of jump frequencies ν depends upon inverse root of the masses M

$$\nu(16)/\nu(18) = \left[M\,(N\bar{O}_3^{18})/M\,(N\bar{O}_3^{16}) \right]^{1/2} = 1{\cdot}05 \qquad (35)$$

Both jump frequency and cage effect which are dependent upon mass provide an explanation of the appearance of large isotope effect at 25°C at which temperature vibrational

frequencies are sufficiently excited. At temperature of —110°C, vibrational excitation is almost absent.

The evidence regarding the nature of diffusing species is provided by the recent work of Cunningham[35]. He has followed the radiolysis at 77 or 300°k by studying reduction of Ce^{4+} in solution and by calorimetric analysis based on diazotisation, the equivalent nitrite contents being $M'(N\overline{O_2})$ and $M(N\overline{O_2})$ respectively. The growth of NO radical concentration as detected by E.P.R. compares favourably with the increase in parameter $[M'(N\overline{O_2})—M(N\overline{O_2})]$ which may represent concentration of nitric oxide $M(NO)$. The additional reactivity towards ceric solution is not affected by thermal or optical bleaching. Similar behaviour is shown by E.P.R. intensity[36] of NO as shown in Fig. 8. These results indicate that radiolysis produces nitric oxide and the oxygen species O_2^- as primary fragment

$$NO_3^- \longrightarrow NO + O_2^- \qquad (36)$$

Among the several possible reaction paths involved in annealing, the following mechanism seems probable

$$NO + O_2^- \longrightarrow (NO_3^-) \longrightarrow NO_2^- + O \qquad (37)$$

The formation[37] of O_2^- in irradiated KNO_3 has been confirmed by E.P.R. studies. Secondary[38,39] product of the reaction is NO_2^- ion. Studies of infra-red absorption, ultraviolet spectra and X-ray diffraction lend support[40,41] to this view. Investigations on kinetics of reformation of nitrate from radiolysis products show that about 16% oxygen in irradiated sample exists as atomic oxygen in close proximity to nitrite ion. The energy barrier for recombination of nitrite ion and atomic oxygen is only 13·0 k calories. The process is unimolecular in nature. Oxygen atoms which penetrate far enough into crystalline lattice combine to produce molecular oxygen. Recombination of molecular oxygen and nitrite ion is a bimolecular process having an activation energy of 31·5 k calories.

Resistance towards radiolysis increases with increase in covalency. In purely ionic compounds such as permanganates defects are produced by multiple ionization of $(MnO_4)^-$ ions. On emission of electron, there is a recoil of the anion. This results in the formation of a reaction site consisting of an interstitial anion and a vacancy. Covalently bonded compounds do not undergo electronic transitions. They possess high resistance towards radiolysis. A severe neutron irradiation can, however, create cluster of defects in these solids. These agglomerates of defects become seats of reaction. These suggestions are supported by the study of cyanamides, which are ionic or covalent compounds. Sodium cyanamide is an ionic compound. Its decomposition occurs on electronic excitation of anion on irradiation. Decomposition of silver cyanamide involves rupture of $Ag\text{-}N$ bond which requires activation energy of 44 k calories per mole. Its resistance towards

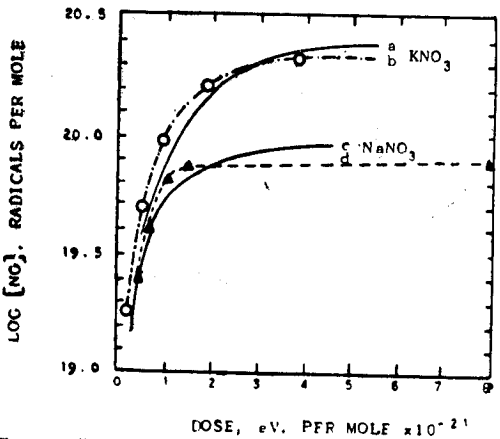

FIG. 8—Growth of the number of nitric oxide radicals formed in KNO_3 and $Na\ NO_3$ by irradiation at 77°K [o...o: exp. methods and —:- chemical methods]

radiolysis by X–rays is high. This is in conformity with its covalent nature. Irradiation[42] with neutrons and fission products reduces induction period to reach acceleratory stage in silver cyanamide.

Chemical reactivity in solids

Thermal decomposition of lead chloride to produce lead and chlorine is simplest to investigate. De Vries and Santen *et al* have investigated[43] the behaviour of lead chloride. A film of pure lead chloride shows a band at 4·66 ev. This may be due to excitation of an electron on the chloride ion or on lead ion. As a reasult of tempering of the film at 330°C for one hour additional hands in the spectrum of the film appear at 4·88, 4·63 and 4·10 ev. Absorption bands at 4·63 and 4·10 ev. may be assigned to colour centres. A proper assignment may throw light on the mechanism of the reaction.

On tempering there is a slight decomposition of $PbCl_2$ which may be described by means of the equation

$$PbCl_2 \longrightarrow Pb + Cl_2 \qquad (38)$$

Chlorine leaves the lattice near the surface giving rise to anion vacancies. This reaction may be represented by means of the equation

$$Cl' \longrightarrow \square_{cl} + \bar{e} + \tfrac{1}{2} Cl_2 \qquad (39)$$

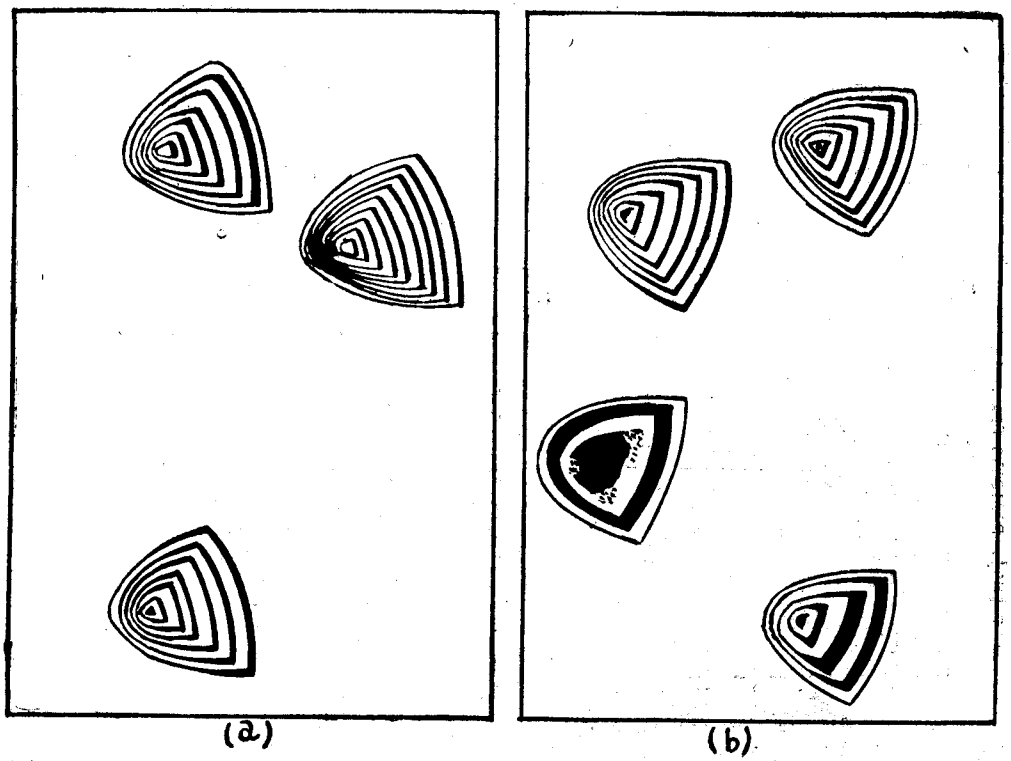

FIG. 9(*a*)—Interferogram of one half of cleaned crystal etched with *d*—Tartaric acid (×320) and (*b*) interferogram of matched half, etched with *l*—Tartric acid (×320)

The electron set free may be trapped at anion vacancy with the formation of F centre which shows absorption at 4·63—4·1 e.v.

$$\square_{cl} + e \longrightarrow \square_{cl}^{-} \qquad (40)$$

Anion vacancies occupying different crystallographic positions may give different types of colour centres.

Chemical reactivity at dislocation sites in calcite has been demonstrated by Thomas & Renshaw[44]. They have observed that large pyramidal pits nucleate at points of emergence of dislocations. A dislocation density of $10^3/cm^2$ on (100) face has been estimated. On etching the top and bottom surfaces with D and L tartaric acid matched, pits on two surfaces appear as shown in Fig. 9. The pits are not mirror image in their shapes. The angle through which a pit is reoriented is the same as the obtuse angle in calcite. Stereospecificity of etching and angle of tilt of the plane containing protruding C-O bonds on the two surfaces account for the observed orientation of pits. In calcite two kinds of dislocations are present, those which glide on (111) plane in [011] direction and those which glide on (100) plane in [011] direction. On etching of heat treated samples, etch pits parallel to short diagonal of rhombohedral faces and parallel to rhomb edge are observed These etch pits indicate the presence of arrays of dislocations and their glide directions.

Earlier Bowden & Singh[45] observed that in metallic azides and fulminates reactions in solid phase occur preferentially along certain crystallographic planes. This is shown in Fig. 10. An appreciable extent of decomposition on these planes may break the crystal into blocks of nearly equal size. An explanation of this interesting observation lies in distribution of dislocations within the crystals and reactvity of the region surrounding each dislocation. Under a thermal stress there is a slip along planes of easy glide and piling up of dislocations on these planes. At elevated temperature dislocations are mobile. Under their mutually repulsive fields, dislocations arrange themselves in regular arrays. The number n of dislocations which accumulate on a plane of lengh L can be estimated[46] by considering the balance between original stress and back stress of generated dislocations. At the point of neutralization of these stresses n is given by the expression

$$n = \pi L\beta\delta/G_m.b \qquad (41)$$

where $\beta \sim 1$, G_m is shear modulus, b is Buerger vector and δ is applied stress. The rate of increase of density of dislocations with strain passes through a maximum at a certain point.

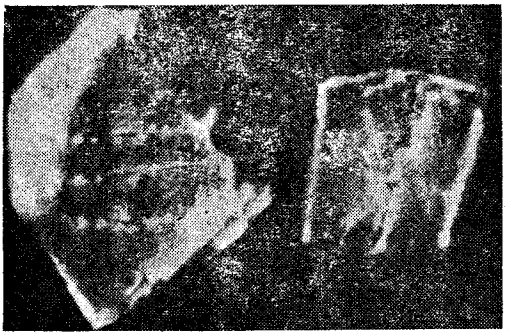

FIG. 10—Split along crytallographic planes in a—leadazide during decomposition.

The stress field around a dislocation is relieved by suitable rearrangement of nearby solute ions or atoms. The gradient of interaction energy provides a force attracting a solute ion to the disolocation. Thermal agitation assists in the migration. A solute ion with polar coordinates r, θ relative to a positive edge dislocation possesses an interaction energy given by the expression[47]

$$E = (A \sin \theta)/r \qquad (42)$$

where A is a constant. As for example E_d is approximately equal to 1 ev for carbon and nitrogen atoms in α— iron. The concentration c of impurity atoms around an edge dislocation at a point where binding energy U is given by

$$c = c_o \exp \frac{-U}{kT} \tag{43}$$

Below a critical temperature Maxwellian distribution is replaced by condensation of solute ions along dislocation lines. The number of solute ions n segregating at time t along dislocation of unit length is given by the expression [48]

$$n = n_o \left(\frac{A D t}{kT}\right)^{\frac{2}{3}} \mu \tag{44}$$

where n_o is initial number of ions in solution per unit volume, D is diffusion coefficient and $\mu \sim 3$.

The mechanism of separation of metallic nuclei at dislocation sites depends upon the type of imperfections present in the crystal. If the sample contains pre-dominantly Frenkel defects Gurney Mott mechanism may account for the formation of nuclei. In case of materials with predominantly Schottky disorder aggregation of charged anion vacancies or F centres may occur. These may coalesce into nuclei. At the dislocations where metallic nuclei appear strain is set up which may be relieved in one of the two possible ways depending upon type of disorder. In materials with Schottky defects the elastic strain is relieved by diffusion of vacancies or divacancies to the site of nuclei. If Frenkel disorder prevails, the strain is relieved by local plastic deformation which results in the formation of additional dislocations. The increase in number of dislocations accelerates the reaction locally. A stage is reached when fracture occurs along the crystallographic planes on which slip occurred in the beginning.

Reactivity of dislocation sites on natural graphite has also been shown by Hennig and Kanter[49]. Screw dislocations of large burger vector occur on most single crystals of natural graphite. Near such dislocations the oxidation rate has been found to be very high.

A good deal of information about reactions in solid phase can be derived from the study of behaviour on irradiation. An irradiated sample of potassium azide shows absorption peaks at 360, 575, 775 and 775 mμ which may be assigned to V, F and R centres respectively. The V centre may consist of complex[50] $(N_3 - N_3)^-$ ion. The observed large width of F-band in KN_3 indicates the coupling of motion of electron in F-centre with internal vibrations of azide ion. An unirradiated sample of potassium azide shows strong absorption at 2002 cm^{-1} in the infra-red which may be assigned to asymmetric vibrations of azide ion. On irradiation at low temperature additional absorption peak [51] at 1637 cm^{-1} appears. This peak has been assigned to a new group which may have the structure $-N=N-N=N-$. On the basis of ESR studies on irradiated potassium azide Shuskus *et al* [52] have also suggested the formation of N_4^- ion. V centres in coloured potassium azide are bleached on irradiation with light of wave length in region of 320-350 mμ. During this irradiation F-centres remain unaffected. Bleaching may be represented by means of reactions given below:

$$(N_3 - N_3)^- \rightarrow 3\,N_2 + e + 2\,\square_{N_3}^- \tag{45}$$

$$(N_3 - N_3) + e \rightarrow 2\,N_3^- \tag{46}$$

Similar reactions may occur on thermal decomposition in other metallic azides. In addition to colour centres metallic nuclei may accelerate chemical reactions on solid surface. Kinetics

of thermal decomposition of lead azide have been studied[53] in detail. Soon after commencement of heating, the crystals are covered with fine metallic nuclei. The reaction in lead azide is initiated by thermal excitation of an electron from azide band to the top of Fermi level of metallic nuclei. On excitation of the electron, hole is left behind in the azide band.

Bimolecular collisions between holes which arrive at the interface leads to evolution of nitrogen

$$2\ N_3 \longrightarrow 3\ N_2 \tag{47}$$

The ions of lead which capture electron go to build up metallic nuclei.

Thermal decomposition of lead azide takes place in three stages. The first stage involves evolution of adsorbed gases which are formed as a result of slow reaction at energetically favourable sites during storage. This is followed by an acceleratory stage. The fractional decomposition α at any time t in this stage may be represented by means of the expression

$$\left(\alpha - \alpha_o\right)^{\frac{1}{n}} = k_l\ (t - t_o) \tag{48}$$

where α, t_o, n and k_l have values of 3·5 % 138 minutes, 2·2 and $5{\cdot}3\times10^{-3}$ /(min)$^{2\cdot2}$ respectively at a temperature of 240·9°C. The maximum rate of decomposition for this isotherm occurs at 220 minutes. There is an inflexion in the curve at this point. The exponential decay may be represented by means of the expression

$$\alpha = \alpha_\infty\ [\ 1 - \exp - k_{l2}\ (t - t'_o)\ ] \tag{49}$$

where α_∞, t'_o have values of 95% and 184·3 minutes respectively at a temperature of 240·9°C. On irradiation of lead azide for 35 hours at a neutron flux of about $7{\cdot}5\times10^{12}$ neutrons/ (cm^2 sec), both induction and accelerating periods become negligible. The rate constant for unirradiated and irradiated lead azide can be represented by the expressions[54]

$$K_{11}\ \text{(unirradiated)} = 10^{12}\ \exp\left(\frac{-36{\cdot}3\text{k calories}}{RT}\right)$$

$$K_{12}\ \text{(irradiated)} = 10^{7\cdot9}\ \exp\left(\frac{-25{\cdot}7\text{k calories}}{RT}\right) \tag{50}$$

where R is gas constant. It is observed that activation energy and pre-exponential factors are lower for the irradiated material than for the un-irradiated sample. The reason for reduction of activation energy is discussed below.

Within the irradiated crystal, clusters of point defects are formed. The ions of lead present around clusters serve as deep traps for electrons which are thermally excited from azide band. The presence of these clusters lowers the activation energy for excitation of electrons from azide band. The energy involved in bimolecular collisions remains unchanged. The total activation energy suffers a fall. Also clusters of defects contain large number of vacant cation sites which serve as traps for the holes. The immobilization of holes near vacant cation sites reduces the probability of collisions between the holes. This reduction in concentration of available holes accounts for the fall in pre-exponential factor. It is interesting to study the factors which determine the rate of reaction in solid azides and to consider the effect of dopants on the rate of decomposition. The successive steps in chemical reactions involving excitation of electrons from the valence to conduction band and the bimolecular interaction between holes can be represented by the equations

$$(N_3)^- \underset{k_{l4}}{\overset{k_{l3}}{\rightleftharpoons}} N_3 + e \tag{51}$$

$$2\,(N_3) \xrightarrow{k_{l5}} 3N_2 \tag{52}$$

The rate of excitation of an electron depends upon lattice vibration and may be represented by means of the expression

$$k_{l3} = \nu \exp \frac{-E_v}{k_T} \tag{53}$$

where ν is frequency of lattice vibration and E_v is the energy involved in hole formation. It may be assumed that ratio of rates k_{l5}/k_{l4} is proportional to ratio ζ_m of mobilities of holes to electrons. The rate constant of interaction between holes is given by the expression

$$k_{l5} = k_{l4}\ \zeta_m\ e^{\frac{-E_h}{k_T}} \tag{54}$$

where E_h is the activation energy involved in interaction between holes. At equilibrium a stationary concentration of holes is built up and the relationship given below holds

$$\frac{d\,(N_3)}{dt} = k_{l3}\ (\bar{N}_3) - k_{l4}\,(N_3)\,(e) - k_{l5}\ (N_3)^2 = 0 \tag{55}$$

since concentration of defects is small, the following conditions are satisfied

$$\begin{aligned} [N_3] &= [e] \\ [N_3] &< \left[\bar{N}_3\right] \\ \left[\bar{N}_3\right] &\simeq N_s \end{aligned} \tag{56}$$

where N_s is number of surafce anions per unit area and [ ] signifies concentration. By making use of the conditions in (55) and (56) it is possible to derive the following relationship

$$[N_3] = \left[\frac{k_{l3}.\ N_s}{k_{l4} + k_{l5}}\right]^{\frac{1}{2}} \simeq \left[\frac{k_{l3}.\ N_s}{k_{l4}}\right]^{\frac{1}{2}} \tag{57}$$

By making use of expressions (54) and (57) it is possible to express the rate constant in the form

$$K_{11} = (\text{constant})\ \ k_{l5}.\ (N_3)^2 = (\text{constant})\ k_{l5}.\left[\frac{k_{l3}.\ k_{l5}.\ N_s}{k_{l4}}\right] - (E_v + E_h)/kT$$

$$\text{or } K_{11} = (\text{constant})\ \zeta_m\ \nu\ N_s\ e \tag{58}$$

The decomposition of heavy[53] metal azide has been observed to follow relationship (58).

Tompkins and Young[55] have studied the thermal decompositon of calcium azide. The reaction may be represented as follows:

$$Ca\,(N_3)_2 \longrightarrow Ca + 3N_2 \tag{59}$$

The temperature coefficient of resistivity of solid product formed in the beginning is positive which is characteristic of metallic state. Semiconductors on the other hand have negative coefficient. This observation is in favour of the assumption that primary solid product of decomposition is clacium metal and not calcium nitride. On subsequent reaction with nitrogen about 18% of metallic calcium transforms into nitride. The decomposition follows a cubic law

$$\alpha^{\frac{1}{3}} = k_{ca}(t - t_o) \qquad (60)$$

This is consistent with three dimensional growth of nuclei. The activation energy is found to be 18 and 35 k calories per mole for well annealed sample and for freshly prepared crystalline mass respectively.

It has been suggested that the fresh sample contains large number of vacancies. The blue coloration at 77°K associated with presence of single anion vacancies has been found to be greatest in freshly prepared sample. On heating, vacancies form into clusters which are nuclei forming sites. On trapping of the electrons or F centres, the clusters transform into metallic nuclei. It is suggested that activation energy of 18 k calories per mole represents true activation energy. The value of 35 k calories in freshly prepared sample arises from variation of pre-exponential factor with temperature. In a fresh sample excess vacancies form into clusters which give additional nuclei. These extra nuclei are responsible for an increase in pre-exponential factor. The effect of pre-irradiation is two-fold. Photolysis produces additional anion vacancies which on clustering give rise to extra nuclei. There is also a decrease in t_o. During irradiation excitons are formed[56] which interact giving rise to photo currents[57] and decomposition. As a result of this embryonic nuclei appear.

Singh[58] has shown that it is possible to sensitize lead azide by incorporation of bismuth in lead azide. This is achieved by the following procedure. 20 cc of 50% solution of ammonium accetate containing 2 cc of 30% hydrazoic acid is saturated with bismuth azide at room temperature. The pH value is adjusted to 6·8. The solution is saturated with lead azide at 70°C. It is allowed to cool when crystals of lead (bismuth) azide appear. The analysis of the product gives 70·7 % lead, 0·24 % bismuth and 28·3 % azide. On incorporation of bismuth in lead azide the temperature of explosion falls by 15·5°C, the impact sensitivity increases by 12 % and activation energy for thermal decomposition decreases by 12 k calories. These results may be explained on the basis of substitutional entry of bismuth in lead azide. This is substantiated by observed absorption in lead (bismuth) azide at a frequency of 1 K. cycle as shown in Fig 11. This absorption may be assigned to orientation of dipole consisting of bismuth Bi^{3+} and cation vacancy in ac field. The sensitization effect may be due to the presence of vacancies which raise the valence band.

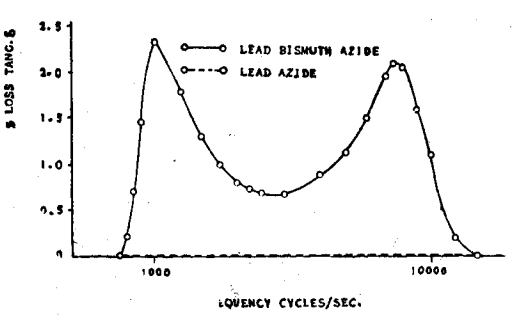

FIG. 11—Difference between loss tangent of lead (Bismuth) azide & lead azide versus frequency.

Another interesting reaction which proceeds in solid phase in organic crystals is the transformation of photo-oxide of anthracene[59] into anthraquinone. The diffraction pattern of the oxide changes progressively even at room temperature due to the following reaction:

$$C_{14}H_{40}O_2 \rightarrow C_{14}H_8O_2 + H_2 \qquad (61)$$

The shape of the molecule is represented in Fig. 12. Photo-oxide is a bent molecule whereas anthraquinone is flat. Oxygen bridge and phenyl wings in photo-oxide undergo rapid vibrations. On the other hand anthraquinone molecule is stable with very little internal motion. The system acquires stability on decomposition. At a temperature of 120°C the evolution of hydrogen is so rapid that explosion occurs.

Recently Mossbauer effect has been used in the study of solid phase reactions. This study has been useful in elucidation of mechanism[60] of oxidation of crocidolite. This is a blue mineral which contains 12·2 % Fe^{3+} and 15·9 % Fe^{2+}. In addition there are silicate ribbons of stoichiometry $Si_{14}O_{11}$. Discrete Mossbauer resonance peaks in crocidolite have been found to be of equal intensity, their chemical shift δ_s and quadrupole splittings Δ are given below

Fe^{2+} $\quad \delta_s = 1{\cdot}20$ mm/sec $\quad \Delta = 2{\cdot}42$ mm/sec.

Fe^{3+} $\quad \delta_s = 0{\cdot}44$ mm/sec $\quad \Delta \simeq 0{\cdot}2$ mm/sec.

It has been suggested that in oxidation electrons jump from Fe^{2+} to Fe^{3+} ions. These electrons, when they arrive at the surface, are trapped by oxygen atoms at the surface. The discreteness of resonances implies that electron jumps occur considerably less frequently than 10^7 sec^{-1}. The oxidized crocidolite contains 27·8% Fe^{3+} and 1·3 % Fe^{2+} and is likely to give one peak due to Fe^{3+}. The Mossbauer spectrum of oxidized product contains two sharply defined lines in close proximity with $\delta_s = 0{\cdot}45$ mm/sec and $\Delta = 1{\cdot}02$ mm/sec. The high quadrupole splitting may be due to ligand effect on symmetric d^3, Fe^{3+} ion.

Catalysis

A catalyst possesses reactivity or selectivity in bringing about chemical reactions. It may either increase the rate of reaction or control the course of the reaction. Adsorption of the reactants and desorption of the products are essential steps in catalysis. Reactants move by diffusion to the surface of the catalyst, combination occurs at the surface, the products and heat of reaction diffuses away from the surface. The bond between the catalyst

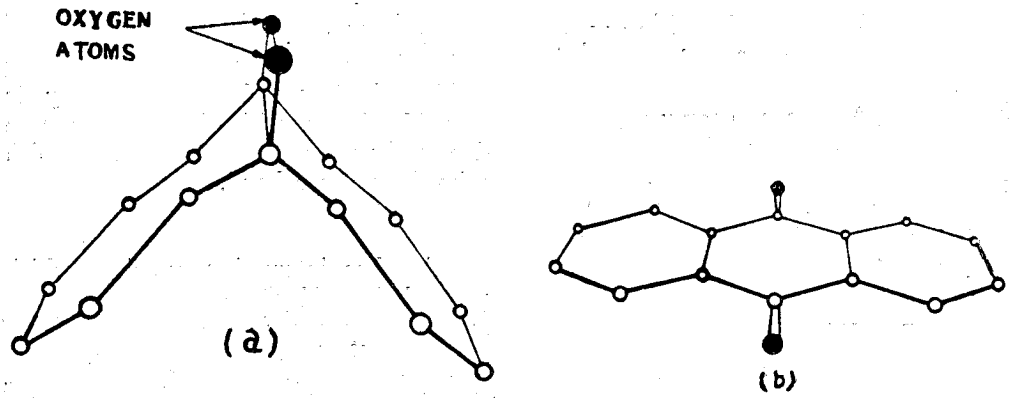

FIG. 12—(*a*) Photoxide of anthracene and (*b*) anthraquinone.

surface and reacting substances should neither be too weak nor too strong. In case of weak bond appreciable adsorption does not occur. A strong bond between the catalyst surface and reactants does not allow escape of the products of reaction. The rate of adsorption is given by the expression

$$dN_a/dt = N^* \; s \; \beta_c \; \epsilon_P \; P \tag{62}$$

where N_a is number of adsorbed molecules, N^* number of adsorption centres per unit area, P is pressure of the gas, s is effective surface area of the adsorbed molecule

$$\beta_c = 1/(2\pi M k T)^{\frac{1}{2}} \tag{63}$$

M is mass of the adsorbed molecule, ϵ_p is probability that a gas molecule arriving at the surface will be adsorbed. In activated adsorption

$$\text{either } \epsilon_p \sim e^{-E_s/kT} \quad \text{or } \overset{*}{N}+ \sim e^{-E_s/kT} \tag{64}$$

where E_s is activation energy for chemisorption. Subsequent to chemisorption, chemical reactions occur. Three types of catalysts are in use (*i*) metallic films (*ii*) semi-conductors and (*iii*) insulators. The mechanisms of their catalytic activity are discussed below:—

Metallic catalysts—On bond formation with reactant molecules, the surface atoms of the metallic catalyst cease to contribute to collective properties of the metal. As for example, magnetism of the nickel power with 20-30A particle size falls on adsorption of the reactant. Similarly, there is a decrease in electrical conductivity on adsorption. The bond between surface and bulk of the atoms of the metals becomes weak on adsorption. Under extreme conditions exposed atoms may dissociate from the surface in the form of a complex. Various faces of the crystal may show different reactivity. The strength of the bond between metallic surface and adsorbed molecule may differ from face to face of the crystal. This difference is associated with closeness of the packing of atoms at a given surface and crystal field stabilization energy.

The decomposition of ammonia on a nickel surface has been investigated by Tamaru, Tanaka, Fukasaku & Ishida[61]. The total uptake of nitrogen by the catalyst has been found to be related to $P_{NH_3}/\sqrt{P_{H_2}}$ indicating the existence of the following equilibrium

$$NH_3 \rightleftharpoons NH_2 \; (a) \; + \; 1/2 \; H_2 \tag{65}$$

where (a) signifies adsorbed species. In the infra-red spectra, bands due to both NH_2 and NH have been detected. At the catalyst surface NH radical may be present in minor amount. During the time of contact the following equilibrium may be attained:

$$2NH_3 \rightleftharpoons 2N \; (a) \; + \; 3H_2 \tag{66}$$

The rate of reaction K_{NH_3} is given by the expression

$$K_{NH_3} = \text{constant } (P^2_{NH_3}/P^3_{H_2}) \; \delta_b \tag{67}$$

The parameter δ_b is related to the strength of the bond between nitrogen and the catalyst and its value is about 0·5. It is the desorption of the nitrogen which controls the reaction rate.

Semiconductor catalysts—Free electrons and holes in the crystal lattice of the semiconductor are important participants in chemisorption and catalysis. As for example in cuprous oxide, Cu and Cu^{2+} sites represent free electrons and holes. These electrons and holes are mobile in the lattice as a result of jump from one atom to the next similar atom. These carriers may be regarded as free valencies which move about the crystal. There is an exchange of free valencies between the surface and bulk of the crystal. The space charge may

be a limiting factor in fresh supply of free valencies. On the basis of this model a semiconducting catalyst emerges as a special kind of polyradical. The physical picture of promotion or poisoning in catalyst consists in control of the concentration of electrons and holes by impurity atoms. In the supply of free carriers to the surface, Fermi level plays the role of a regulator of chemisorption and catalytic properties of the surface. As for example, in ZnO there is direct relationship between electrical conductivity and activity, it may promote dehydrogenation or dehydration depending upon its band structure.

The dehydrogenation reaction involves removal of hydrogen

$$C_2H_5\ OH \xrightarrow{ZnO} CH_3\ CHO\ + H_2 \tag{68}$$

The initial step may be the rupture of $O—H$ bond

$$CH_3\ CH_2\ OH \xrightarrow[ZnO]{} CH_3CH_2O\ (a)\ +\ H\ (a) \tag{69}$$

where symbol (a) implies adsorbed state. This may be followed by two consecutive reactions

$$CH_3\ \ CH_2\ O\ (a) + H(a) \rightarrow CH_3\ \overset{1}{C}HO\ (a)\ + H_2 \tag{70}$$

$$CH_3\ \overset{1}{C}HO\ (a) \rightleftharpoons CH_3\ \overset{H}{\overset{1}{C}} = O\ (\text{gas}) \tag{71}$$

Impurities which displace the Fermi level in ZnO upwards promote hydrogenation. ZnO containing excess[62] zinc in the form of interstitial Zn^+ ions and free electrons is a good catalyst for this reaction. The additions[63] to zinc oxide of impurities which lower its Fermi level help in dehydration reaction

$$C_2H_5\ OH \xrightarrow{ZnO} \begin{matrix} CH_2 \\ \| \\ CH_2 \end{matrix} + H_2O \tag{72}$$

The rates of reactions in two cases may be represented in the forms

$$K\ (\text{dehydrogenation}) = \text{constant}\ P.\ e^{-('E - \overset{+}{\epsilon_s})/kT} \tag{73}$$

$$K\ (\text{dehydration}) = \text{constant}\ P\ e^{-(''E - \overset{-}{\epsilon_s})/kT} \tag{74}$$

where $^+\epsilon_s = (E_g - {}^-\epsilon_s)$ is Fermi level, E_g is forbidden energy gap, P is pressure of alcohol, $'E$ and $''E$ are ionization energies.

Oxidation of carbon monoxide on p type NiO provides an interesting example of a semiconducting[64] type of catalyst. The reaction is first order with respect to partial pressure of carbon monoxide and zeroth order with respect to partial pressure of oxygen which is adsorbed to a high coverage with high heat of adsorption. In contrast to this strength of bond between carbon monoxide and the catalyst is low. This may be due to limited overlap between electronic orbitals on carbon monoxide and dz^2 orbital of nickel. The chemisorption of CO on the catalyst is limited and rate of chemisorption determines the rate of reaction.

The first step in the chemisorption of CO is the transfer of an electron from the gas to the surface of the catalyst

$$CO \rightleftharpoons CO^+(a)\ +\ e\ (a) \tag{75}$$

where (*a*) implies interaction with the oxide catalyst. The electrons go to fill up the bands in the 3*d* levels of Ni^{2+} ions, which results in a reduction in conductivity of the oxide. The adsorbed oxygen molecules trap electrons from nickel ions and regenerate holes. A complex $Ni^{3+} - O_2^-$ is formed at the adsorption site and is responsible for reversible adsorption of oxygen. The adsorbed O_2^- ion may break-up into oxygen ions by capturing an electron from another Ni^{2+} ion if it happens to be in close proximity. The fraction of oxygen molecules which suffer dissociation are irreversibly adsorbed. It is existence of pairs of Ni^{2+} ions near an anion vacancy which is responsible for irreversible adsorption. The electronic levels corresponding to $\bar{O}$ ions lie well below the Fermi level of pure oxide. The irreversible dissociation may be represented by the expression

$$\tfrac{1}{2}\, O_2\,(\text{gas}) + \overset{2+}{Ni} + \square_{Ni}{}^{2+} \longrightarrow \bar{O}\,(a) + \overset{3+}{Ni} \,\text{X}\, \square_{Ni}{}^{2+} \qquad (76)$$

where $Ni^{3+} \,\text{X}\, \square_{Ni}{}^{2+}$ is nickel ion with trapped hole associated with a cation valency. The adsorbed carbon monoxide reacts with adsorbed oxygen to form $CO_3{}^{2-}$ complex. The slope of linear plot representing[65] amount of irreversibly adsorbed carbon monoxide versus amount of pre-adsorbed oxygen suggests that $CO_3{}^{2-}$ complex is formed. Dissociating of this complex by thermal excitation completes the reaction.

The reactivity of nickel oxide may be increased by incorporation of lithium and decreased by addition of chromium. The activation energies for oxidation on pure nickel oxide, the oxide containing 2·5 per cent lithium and the oxide with 5 per cent chromium, are 14·0, 11·5 and 17·6 k calories respectively. The corresponding logarithms of the pre-exponential factors are 4·0, 3·2 and 4·7 respectively. The increase in the rate by addition of lithium and decrease in the rate by addition of chromium arise from changes in concentration of holes

$$Li_2O + 1/2\; O_2{}^- \rightarrowtail 2\, Li_{Ni}^{+} + 2^{+} h + 2\; \bar{\bar{O}}\,(\text{matrix}) \qquad (77)$$

$$Cr_2\; O_3 + 2\overset{+}{h} \rightleftharpoons 2\; \overset{3+}{Cr_{Ni}} + \tfrac{1}{2}\; O_2\; (g) + 2\,\bar{O} \qquad (78)$$

If $Ni\,O$ is irradiated[66] with neutrons, F centres are formed which help in the transfer of an electron from $\overset{2+}{Ni}$ to oxygen atoms.

Insulating compounds—Ions with multiple charges in ionic insulators such as Al^{3+} in Al_2O_3 exert a powerful polarising force on bonds in the reactants. This helps in rupture of the bond and speeding up of the reaction. The reactivity of the oxide may be increased by special treatment. In mixed oxide of silicon and aluminium, Al^{3+} ions may replace Si^{4+} ions. The electro-neutrality may be attained by trapping up of protons as shown below:

$$\begin{array}{ccccccc} H^+ & & & & (a) & & C \\ O & : & Al & : & O & : & Si \\ & & \vdots & & & & \vdots \\ & & O & & & & O \end{array} \quad : \; O$$

The isomerization of butene on this catalyst may be represented as follows:

$$\overset{+}{H}(a) + CH_2 = CH\; CH_2\; CH_3(a) \rightleftharpoons H_3\; C\; CH\; CH_2\;\; CH_3\;(a) \qquad (79)$$

$$CH_3\; CH\; CH_2\; CH_3\;(a) \longrightarrow CH_3\;\; CH = CH\; CH_3 + \overset{+}{H}\,(a) \qquad (80)$$

The nature of active sites on alumina-silica catalyst has been investigated by Basila, Kantner & Rhee[67]. They have examined the infra-red spectra of pyridine adsorbed

on its surface. The presence of bands corresponding to pyridinium ion and pyridine in the adsorbate indicates the existence of both Bronsted (H_a^+) and Lewis (electron pair acceptor) acidic sites in equal number on the surface of the catalyst. Both types of centres are active in catalyst.

Defect oxides contain vacant sites on the surface as is the case in defect Cr_2O_3 where vacancies occur on one of the octahedral sites. The existence of charged vacant sites builds up catalytic activity. Ziegler-Natta catalyst also falls in this category and mechanism of its action is discussed below.

Polymerization of propene on solid catalyst consisting of α—$TiCl_3$ and AlR_3 gives highly stereoregular[68] chains which have same configuration of asymmetric carbon atom throughout polymer chain. The active sites on the surface of such solid catalyst are octahedrally coordinated ions of transition metal. These ions possess t_{2g} orbitals which may be empty or partially empty. Out of the six octahedral positions, four may be occupied by the chlorine atoms, one position above the surface may be occupied by the alkyl group and the sixth position on the surface may be vacant. Steric hindrance determines the orientation of propene. Methyl group is bulky. Any easy way of inserting the monomer into vacant site may be the one in which CH_2 group points into the lattice. The double bond in the propene molecule tends to form a π-bond with t_{2g} orbital in Ti^{3+} ion. This bond retains propene molecule in a suitable orientation. Under thermal lattice vibration alkyl group on the adjacent position attaches itself to carbon atom of propene molecule. The reaction may be written as in Fig. 13.

According to this mechanism catalytic activity and low activation energy are primarily due to the size of the orbital of the transition metal. The polymer grows by oscillation between two octahedral positions which are occupied by an alkyl group and chlorine vacancy. It is the defect structure of solid alkylated $TiCl_3$ which controls the isotacticity of the polymer.

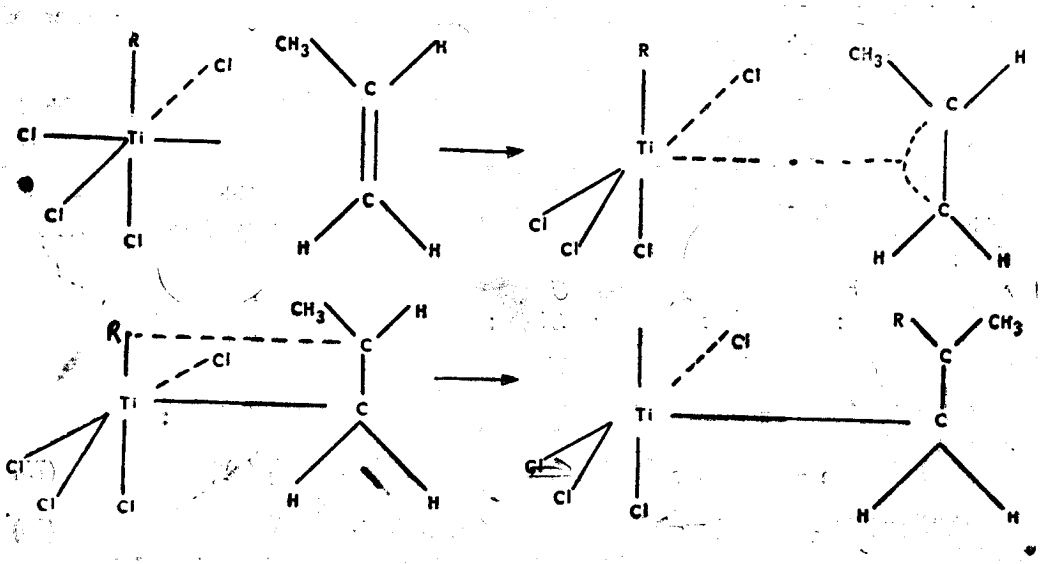

FIG. 13—Polymerization of propene.

CONCLUSION

Mechanisms of reactions involved in photolysis, radiolysis, catalyst and in other solids have given valuable information regarding reactivity in solids. The importance of the study of electronic band structure, energetics of mass transfer, mechanism of electronic and atomic motion, and methods of control of imperfections has been brought out. There are gaps in our knowledge regarding most of these aspects. A programme of investigations on reactivity of pure and suitably doped compounds will be rewarding.

REFERENCES

1. SHANNON, R.D., *Trans. Faraday Soc.*, **60** (1964), 1902.
2. TAFT, E.A., PHILLIP, H.R. & APKER, L., *Phys. Rev.*, **110** (1958), 876.
3. BROWN, F.C., MASUMI, T. & TIPPINS, H.H., *J. Phys. Chem. Solids*, **22** (1961), 101.
4. CARROLL, B.H., KRETCHMANN, C.M., *J. Res. Natl. Bur. Std.*, **10** (1933), 449.
5. GILLEO, M.A., *Phys. Rev.*, **91** (1953), 534.
6. HOWLAND, L.P., *ibid.*, **109** (1958), 1927.
7. TIPPINS, H.H. & BROWN, F.C., *Bull. Amer. Phys. Soc.*, **7** (1962), 221.
8. OKAMOTO, Y., *Nachr. A. Kad. Wiss. Gottingen*, **14** (1956), 275.
9. BROWN, F.C., *J. Phys. Chem.*, **66** (1962), 2368.
10. DEREYSER, W., "Proc. 4th Internat. Symp. on Reactivity of Solids 1960". Edited by J. H. DE BOER *et. al.* (Elsevier Publishing Co., Amsterdam) 1961, p. 376.
11. CHRISTY, R.W. & PHELPS, D.H., *Phys. Rev.*, **124** (1961), 1053.
12. COHEN, M.H., KANZIG, W. & WOODRUFF, T.O., *J. Phys. Chem. Solids*, **11** (1959), 120.
13. TELTOW, J., *Ann. Phys.* (Leipzig), **5** (1949), 71.
14. KURNIK, S.W., *J. Chem. Phys.*, **20** (1952), 218.
15. KROGER, F.A., *J. Phys. Chem. Solids*, **26** (1965), 901.
16. HANSON, R.C., *J. Phys. Chem.*, **16** (1962), 2376.
17. ILSCHNER, B., *ibid.*, **28** (1958), 1109.
18. HANNAY, N.B., "Semi Conductors" (Reinhold, New York) 1959, p. 331.
19. LAYER, H. & SLIFKIN, L., *J. Phys. Chem.*, **66** (1962), 2396.
20. LAWSON, A.W., *Phys. Rev.*, **78** (1950), 185.
21. KANZAKI, H., *ibid.*, **81** (1951), 884.
22. LAWSON, A.W. & CHRISTY, R.W., *J. Chem. Phys.*, **10** (1951), 517.
23. SHAPIRO, I. & KOLTHOFF, I.M., *ibid.*, **15** (1947), 41.
24. KURNICK, S.W., *ibid.*, **20** (1952), 218.
25. LIDIARD, A.B., *Handbuch der Physik.*, Springer-Verlag, Berlin, **20** (1957), 246.
26. MCCOMBIE, C.W. & LIDIARD, A.B., *Phys. Rev.*, **101** (1956), 1210.
27. FRIAUF, R.J., *J. Phys. Chem.*, **66** (1962), 2380.
28. BOND, W.L. & KAISER, W., *J. Phys. Chem. Solids*, **16** (1960), 44.
29. BRINDLEY, G.W. & HAYARNI, R., *Phil., Mag.*, 12 (1965), 505.
30. HLAVAC, J., "Proc. 4th Internat. Symp. on Reactivity of Solids 1960". Edited by J.H. DE BOER *et. al.* (Elsevier Publishing Co., Amsterdam), 1961, p. 129.
31. HEDGES, J.M. & MITCHELL, J.W., *Phil. Mag.*, **44** (1953), 357.
32. MITCHELL, J.W., *J. Phys. Chem.*, **66** (1962), 2359.
33. GURNEY, R.W. & MOTT., N.F., *Proc. Roy, Soc.* London, **164A** (1938), 151.
34. CUNNINGHAM, J., *J. Phys. Chem.*, **65** (1961), 628.
35. ———, *ibid.*, **67** (1963), 1772.
36. ———, *J. Phys. Chem. Solids*, **23** (1962), 843.
37. ———, *J. Phys. Chem.*, **66** (1962), 779.
38. JOHNSON, E.R., *J. Amer. Chem. Soc.*, **80** (1958), 4460.
39. MADDOCK, A.G. & MOHANTY, S.R., *Discussion Faraday Soc.*, **31** (1961), 193.
40. CUNNINGHAM, J. & HEAL, H.G., *Trans. Faraday. Soc.*, **54** (1958), 1355.
41. PRINGSHEIM, *J. Chem. Phys.*, **23** (1955), 369.
———, *ibid.*, **23** (1955), 1113.

42. SOLE, M.J. & JOFFE, A.D., *Proc. Roy. Soc.*, **277A** (1964), 523.
43. VRIES, K. J. DE & VAN-SANTEN, J.H., *Physica*, **30** (1964), 2051.
MIMKOVICH, G.J., *Phys. Chem. Solids*, **24** (1963), 213.
44. THOMAS, J.M. & RENSHAW, G.D., *Trans. Faraday Soc.*, **61** (1965), 791.
45. BOWDEN, F.P. & SINGH, K., *Proc. Roy. Soc.*, **227A** (1954), 22.
46. ESHELBY, J.D., FRANK, F.C. & NABARRO, F.R.N., *Phil. Mag.*, **42** (1951), 351.
47. COTTRELL, A.H., "Progress in Metal Physics Vol I" (Butterworth) 1949, p. 77.
48. ————, & BILBY, B.A., *Proc. Phys. Soc.*, 62A (1949), 49.
49. HENNING, G.R. & KENLER, M.A., "Proc. 4th Internat. Symp. on Reactivity of Solids 1960" Edited by J.H. DE BOER *et. al.*, (Elsevier Publishing Co., Amsterdam) 1961, p. 649.
50. HEAL, H.G. & PRINGLE, J.P.S., *J. Phys, Chem. Solids*, **15** (1960), 261.
51. PAPAZIAN, H.A., *ibid.*, **21** (1961), 81.
52. SHUSKUS, A.J., YOUNG, C.O., WILLIAM, O.R. & LEVY, P.W., *J. Chem. Phys.*, **33** (1960), 622.
53. GRIFFITHS, P.J.F. & GROCOCK, J.M., *J. Chem. Soc.* August (1957), 3380.
54. JACH. J., *Trans. Faraday Soc.*, **59** (1963), 947.
55. TOMPKINS, F.C. & YOUNG, D.A., *ibid.*, **61** (1965), 1470.
56. DEB, S.K., *ibid.*, **59** (1963), 1414.
57. ————, *ibid.*, **59** (1963).
58. SINGH, KARTAR, To be communicated.
59. BREE, A., LYONS, L.E., *J. Chem. Soc.*, December (1960), 5170.
60. GIBB, T.C. & GREENWOOD, N.N., *Trans. Faraday Soc.*, **61** (1965), 1317.
61. TAMARU, K., TANAKA, K., FUKASAKA, S. & ISHIDA, S., *ibid*, **61** (1965), 765.
62. KRYLOV, O.V., ROGINSKI, S.Z. & FOKINA, YE. A., *Izv Akad. Nauk. SSSR.*, Chemistry Section (1957), 422.
63. VLADIMIROVA, V.N., YENIKEYEV, E. KH., ZHABROVA, G.M., & MARGOLIS, L.YA., *Dokl. Akad. Navk SSSR*, 131 (1960), 342.
64. DRY, M.E. & STONE, F.S., *Discussion Faraday Soc.*, **28** (1959), 192.
65. COTTON, J.D. & FENSHAM, P.J., *Trans. Faraday Soc.*, **59** (1963), 1444.
66. CHARMAN, H.B. & DELL, R.M., *ibid.*, 59 (1963), 470.
67. BASILA, M.R., KANTNER, T.R., & RHEE, K.H., *J. Phys. Chem.*, **67** (1951), 3197.
68. COSSEE, P., *Trans. Faraday Soc.*, **58** (1962), 1226.